Compact high-resolution differential interference contrast soft x-ray microscopy

Michael C. Bertilson,[1,a)] Olov von Hofsten,[1] Magnus Lindblom,[1] Thomas Wilhein,[2] Hans M. Hertz,[1] and Ulrich Vogt[1]

[1]*Biomedical & X-Ray Physics, Department of Applied Physics, Royal Institute of Technology/AlbaNova, SE-106 91 Stockholm, Sweden*
[2]*University for Applied Sciences, RheinAhrCampus Remagen, Suedallee 2, D-53424 Remagen, Germany*

We demonstrate high-resolution x-ray differential interference contrast (DIC) in a compact soft x-ray microscope. Phase contrast imaging is enabled by the use of a diffractive optical element objective which is matched to the coherence conditions in the microscope setup. The performance of the diffractive optical element objective is evaluated in comparison with a normal zone plate by imaging of a nickel siemens star pattern and linear grating test objects. Images obtained with the DIC optic exhibit typical DIC enhancement in addition to the normal absorption contrast. Contrast transfer functions based on modulation measurements in the obtained images show that the DIC optic gives a significant increase in contrast without reducing the spatial resolution. The phase contrast operation mode now available for our compact soft x-ray microscope will be a useful tool for future studies of samples with low absorption contrast. © *2008 American Institute of Physics*. [DOI: 10.1063/1.2842422]

X-ray microscopy is a high-resolution imaging method with nanometer-scale resolution using diffractive zone plates as microscope objectives.[1] Synchrotron radiation sources are the preferred light sources for most of today's existing x-ray microscopes; however, there is a growing interest in so-called compact instruments. These employ the x-ray emission of laser-generated plasmas and can be built as compact as the size of an optical table, thereby allowing the operation in a laboratory environment. Recently, we demonstrated the second generation of our compact soft x-ray microscope which is capable of resolutions down to 30 nm.[2] A drawback of compact x-ray microscopes is the relatively low number of x-ray photons available for the imaging process. In order to improve image contrast or to reduce exposure times, the use of phase contrast in addition to the normal absorption contrast is of great benefit. For hard x rays, where the penetration depth is much longer, phase contrast x-ray imaging is even more important. In the present publication, we present a compact nanometer-resolution x-ray microscope which is capable of differential phase contrast imaging by the use of a specially designed diffractive optical element (DOE) objective.

High-resolution phase contrast x-ray microscopy has been demonstrated by Zernike phase contrast[3–5] and differential interference contrast (DIC).[6–8] The latter has the advantage that only the zone plate objective in the microscope has to be replaced by a special optic that provides the DIC effect. DIC imaging uses the superposition of two images and the so-called shear and bias are used to control image contrast. The shear is the separation between the images and the bias is a constant phase retardation introduced to one of the images. So far, two types of optics have been used for this purpose, a so-called twin zone plate[9] consisting of two slightly shifted identical zone plates or a single DOE.[7,10] Since the fabrication and alignment of a single DOE optic is much easier than that of a twin zone plate, we chose the single DOE approach for our compact microscope. The pattern of a DIC DOE can be calculated in different ways, based on Fourier[11] or holographic[8,10] approaches. Both methods lead to the same type of pattern, which is essentially zone-plate-like but in which lines and spaces are interchanged in certain parts of the optic (see Fig. 1 for examples). We call the position where the change takes place for a phase cut.

In order to get differential interference in the image, one carefully has to consider the object illumination conditions, since the DIC effect will depend on the spatial coherence in the object plane. In compact x-ray microscopy, the microscope condenser can be treated as a secondary source consisting of mutually incoherent but individually coherent emitters which fully determines the spatial coherence in the
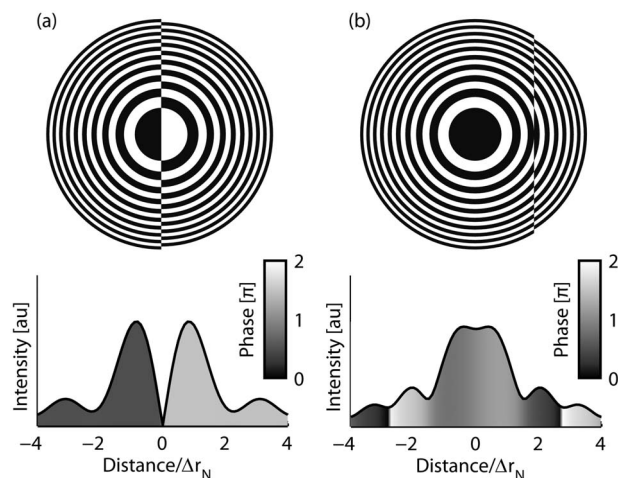

FIG. 1. An illustration showing the basic pattern of two types of DIC DOEs and their corresponding PSFs. The only difference between the optics is the position of the phase cut. The corresponding PSF intensities are presented (continous lines) together with the PSF intensity of a normal zone plate (dashed lines). Shadings under the graphs show the relative phase of the PSFs.

a)Electronic mail: michael.bertilson@biox.kth.se.

object plane.[12] A sufficient degree of coherence is needed over the shear distance for the images to interfere, which can be observed in the point spread function (PSF). In Fig. 1(a) a possible DOE pattern for DIC microscopy[7,13] is shown together with its calculated intensity PSF in the horizontal direction, which is the direction of shear. Also shown is the PSF for a normal zone plate (in dashed). The two spots are separated approximately $2\Delta r_n$, where Δr_n is the outermost zone width and therefore also approximately the resolution of a normal zone plate optic. However, this distance will not be coherently illuminated in our compact microscope. Accordingly, images taken by the microscope with this type of optic showed no DIC effect. Instead, a double image was clearly visible in the direction of the shear, reducing the spatial resolution.

We have calculated a DIC DOE, from now on referred to as the side-cut DOE, matched to the coherence conditions in our compact microscope that shows no decrease in spatial resolution. This is enabled by a shear close to the resolution limit of the objective. The calculated intensity PSF and the optic are shown in Fig. 1(b). An even smaller shear could be achieved by placing the phase cut further to the side, but calculations showed that this had a negative effect on the DIC image. Also visible in Fig. 1 is the phase of the PSFs indicated by relative shading. The phase difference over the shear distance corresponds to the bias of the optic. The two optics illustrated in Figs. 1(a) and 1(b) show a bias equal to π and $\pi/2$, respectively. As shown in the figure, both the shear and the bias are affected when moving the phase cut in the optic. The wider intensity PSF compared to a normal zone plate does not necessarily imply lower resolution. Since the phase changes over the spot separation, the resolution will be close to the shear rather than to the width of the PSF, if the degree of coherence over the shear is sufficient. A theoretical background explaining how the optic was calculated and the correlation between DIC image contrast and degree of spatial coherence as well as bias is given in a separate publication.[14]

We fabricated a prototype of the side-cut DOE for an initial experiment allowing us to see if the expected phase contrast could be obtained. It was fabricated along with a normal zone plate in nickel on a 50 nm Si_3N_4 supporting membrane using e-beam lithography and a following nanofabrication process.[15] Both optics have an outermost zone width of 50 nm, an average zone height of $\sim$100 nm, and a diameter of 75 μm giving $N=375$ zones and a focal length of 1.5 mm at $\lambda=2.48$ nm. The side-cut DOE was tested as objective in the second generation of our compact soft x-ray microscope[2] which utilizes the predominant emission line at $\lambda=2.48$ nm of a liquid-nitrogen-jet target laser-plasma soft x-ray source[16] with a source size of 20 μm at full width at half maximum and a spectral bandwidth of $\lambda/\Delta\lambda>500$.[17]

The microscope uses critical illumination via 1:1 imaging of the source onto the sample with a central-stop-equipped nickel condenser zone plate (CZP).[18] The CZP has an outer diameter of 4.53 mm, an inner diameter of 3.75 mm, and the outer zone width is $\Delta r_N=49$ nm, giving a first order focal length of 90 mm at $\lambda=2.48$ nm. The combination of the CZP, central stop, and a pinhole in front of the sample plane acts as a monochromator making sure that the temporal coherence requirement $\lambda/\Delta\lambda>N$, where N is the number of zones, is met. The coherently illuminated area on the CZP is less than 16 μm^2, thus it can be considered inco-
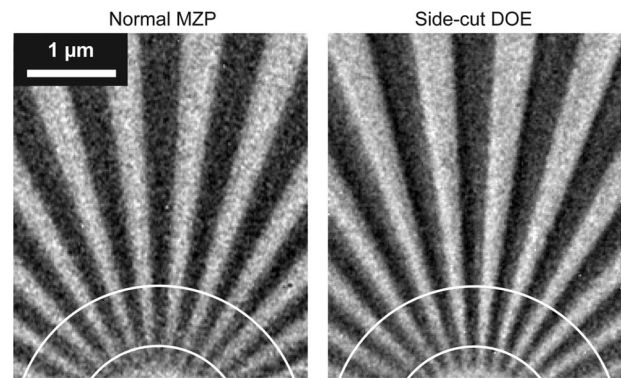

FIG. 2. The figure shows the same region of the siemens star test object imaged by a normal zone plate and by the side-cut DOE. The contrast mechanism is clearly different in the two images. The left is based on absorption contrast, whereas the right image exhibits a strong DIC edge enhancement in addition to the ordinary absorption contrast.

herently illuminated. According to the van Cittert-Zernike theorem, the degree of coherence over the side-cut DOE spot separation in the sample plane of our microscope is $\sigma=0.53$.

Since the optics membrane includes both the side-cut DOE and a normal zone plate, the switching of the imaging optic can be done by simply moving the source in the vertical direction and no time consuming realigning of the microscope is necessary. This enables easy comparison of the two optics.

Images were acquired with an objective-to-detector distance of 1100 mm giving a magnification of $\sim$730 which is sufficient for resolving the expected DIC edge effect. All other components of the arrangement are identical to that of the normal operation of the microscope.[2]

The performance of the side-cut DOE, as in its ability to produce DIC images, was investigated by comparing its imaging properties with those of the normal zone plate. As a test object, an in-house-fabricated nickel siemens star with an inner most period of 150 nm and an average spoke thickness of 90 nm was used. This object contains several spatial frequencies and the thickness of the spokes provides a sufficient phase shift, $\sim\pi/3$ rad, making it a suitable test object for phase contrast optics. Linear nickel gratings with 200, 160, and 100 nm periods were also imaged in order to do more reliable contrast comparisons for higher spatial frequencies.

The performance of the normal zone plate and the side-cut DOE is exemplified in Figs. 2 and 3. Figure 2 shows cropped images of the same region of the siemens star test
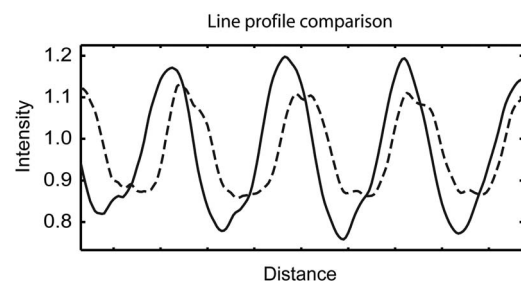

FIG. 3. Comparison of average edge profiles obtained with the side-cut DOE (continuous line) and the normal zone plate (dashed line), measured between the two radii marked in Fig. 2 with spatial frequencies between 3 and 5 μm^{-1}.
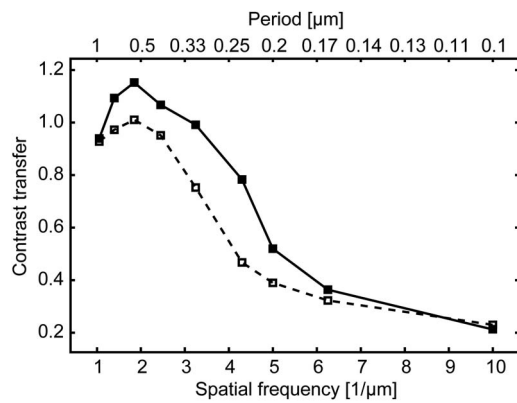
FIG. 4. Contrast transfer functions of the side-cut DOE (continuous line) and the normal zone plate (dashed line) based on experimental data. These curves show that this type of DOE gives an enhanced contrast. Notice the maximum contrast increase by a factor of 2 at around 4 μm^{-1}.

object mentioned above. Figure 3 shows the average edge profile, in the direction where the contrast increase is most prominent, for spatial frequencies between 3 and 5 μm^{-1}, measured between the two radii marked in Fig. 2. As seen in these two figures, the contrast mechanism clearly differs between the two objectives. The left image in Fig. 2 exhibits ordinary absorption contrast, whereas the right image exhibits typical DIC phase contrast in addition to the normal absorption contrast. This is seen as dark and bright edge enhancements in the direction of the shear corresponding to positive and negative phase gradients in the sample. This DIC characteristic proportionality between the intensity profile and the phase gradient of the sample is even more clearly demonstrated in Fig. 3. Similar edge effects can be obtained in transmission microscopy using only parts of the full condenser aperture, i.e., oblique illumination, and can, if the illumination conditions are not considered, be mistaken for DIC. The different effects can be distinguished since the direction of the edge contrast enhancement is, in the case of oblique illumination, related to the orientation of the oblique illumination, but in the case of DIC it is related to the direction of shear in the optic. To verify that the edge effect was DIC, a series of images with oblique illumination were acquired by moving the source along the direction of shear from one side of the optical axis to the other. The edge effect was never inverted, which would have been the case if it was based on the illumination. Therefore, one can conclude that the effect is based on DIC. Furthermore, the strength of the DIC effect was found to be sensitive to the alignment of the illumination which is expected.

To quantify the contrast enhancement obtained with our side-cut DOE the modulation at different radii of the siemens star images as well as the modulation in the grating images were measured after which they were normalized using the expected absorption contrast modulation, $m=0.25$, of a binary structure of 90 nm thick nickel features. Based on these measurements, we plotted the contrast transfer for the two objectives as a function of spatial frequency shown in Fig. 4. This figure shows that the side-cut DOE gives a significant increase in contrast compared to a normal zone plate. Notice that the maximum contrast, increased by a factor of 2 for frequencies around 4 μm^{-1}, is also demonstrated in Fig. 3. Ideally, as when the resolution is diffraction limited, the relative contrast increase reaches a maximum for lines and

spaces equal to the shear distance, which, in our case, corresponds to 10 μm^{-1}. However, the resolution of the optic is not diffraction limited which causes a decreased relative contrast gain for spatial frequencies approaching the resolution limit of the optic. The expected maximum contrast increase could therefore not be observed. The observed difference in modulation in the images of the 100 nm period grating is smaller than 0.008 which is within the expected measurement error. Therefore, these results show that both optics resolve the 100 nm period grating without a measurable difference in contrast. Hence, the important finding from the comparison is that the side-cut DOE gives an increased contrast without reducing the spatial resolution.

We have presented nanometer-resolution differential phase contrast images obtained in a compact soft x-ray microscope using a single-element optic. The phase contrast operation mode now available for our compact soft x-ray microscope will be of interest for future studies of low absorption contrast samples. This optic does not place any extra limitation on the fabrication process, making it available for recently presented 15 nm zone plate technology. In addition, the side-cut DOE is also applicable to synchrotron-based instruments, where applications include hard x-ray phase contrast microscopy[5] and magnetic phase contrast microscopy.[7] In these fields, we anticipate that our side-cut DOE optic can provide complementary results to existing Zernike phase contrast techniques.

[1] W. Chao, B. D. Harteneck, J. A. Liddle, E. H. Anderson, and D. T. Attwood, Nature (London) **435**, 1210 (2005).
[2] P. A. C. Takman, H. Stollberg, G. A. Johansson, A. Holmberg, M. Lindblom, and H. M. Hertz, J. Microsc. **226**, 175 (2007).
[3] G. Schmahl, D. Rudolph, G. Schneider, P. Guttmann, and B. Niemann, Optik (Jena) **97**, 181 (1994).
[4] G. Schmahl, D. Rudolph, P. Guttmann, G. Schneider, J. Thieme, and B. Niemann, Rev. Sci. Instrum. **66**, 1282 (1995).
[5] U. Neuhausler, G. Schneider, W. Ludwig, M. A. Meyer, E. Zschech, and D. Hambach, J. Phys. D **36**, 79 (2003).
[6] T. Wilhein, B. Kaulich, E. Di Fabrizio, F. Romanato, S. Cabrini, and J. Susini, Appl. Phys. Lett. **78**, 2082 (2001).
[7] C. Chang, A. Sakdinawat, P. Fischer, E. H. Anderson, and D. T. Attwood, Opt. Lett. **31**, 1564 (2006).
[8] U. Vogt, M. Lindblom, P. A. C. Jansson, T. T. Tuohimaa, A. Holmberg, H. M. Hertz, M. Wieland, and T. Wilhein, Opt. Lett. **30**, 2167 (2005).
[9] B. Kaulich, T. Wilhein, E. Di Fabrizio, F. Romanato, M. Altissimo, S. Cabrini, B. Fayard, and J. Susini, J. Opt. Soc. Am. A **19**, 797 (2002).
[10] E. Di Fabrizio, D. Cojoc, S. Cabrini, B. Kaulich, J. Susini, P. Facci, and T. Wilhein, Opt. Express **11**, 2278 (2003).
[11] C. Chang, P. Naulleau, E. Anderson, K. Rosfjord, and D. Attwood, Appl. Opt. **41**, 7384 (2002).
[12] O. von Hofsten, P. A. C. Takman, and U. Vogt, Ultramicroscopy **107**, 604 (2007).
[13] M. Lindblom, T. Tuohimaa, A. Holmberg, T. Wilhein, H. M. Hertz, and U. Vogt, Spectrochim. Acta, Part B **62**, 539 (2007).
[14] O. von Hofsten, M. Bertilson, and U. Vogt, Opt. Express **16**, 1132 (2008).
[15] A. Holmberg, S. Rehbein, and H. M. Hertz, Microelectron. Eng. **73-74**, 639 (2004).
[16] P. A. C. Jansson, U. Vogt, and H. M. Hertz, Rev. Sci. Instrum. **76**, 043503 (2005).
[17] T. Wilhein, D. Hambach, B. Niemann, M. Berglund, L. Rymell, and H. M. Hertz, Appl. Phys. Lett. **71**, 190 (1997).
[18] S. Rehbein, A. Holmberg, G. A. Johansson, P. A. C. Jansson, and H. M. Hertz, J. Vac. Sci. Technol. B **22**, 1118 (2004).